

BagPipe: Accelerating Deep Recommendation Model Training

Saurabh Agarwal
agarwal@cs.wisc.edu

Chengpo Yan
cyan46@wisc.edu

Ziyi Zhang
zzhang765@wisc.edu

Shivaram Venkataraman
shivaram@cs.wisc.edu

University of Wisconsin-Madison

Abstract

Deep learning based recommendation models (DLRM) are widely used in several business critical applications. Training such recommendation models efficiently is challenging primarily because they consist of billions of embedding-based parameters which are often stored remotely leading to significant overheads from embedding access. By profiling existing DLRM training, we observe that only 8.5% of the iteration time is spent in forward/backward pass while the remaining time is spent on embedding and model synchronization. Our key insight in this paper is that access to embeddings have a specific structure and pattern which can be used to accelerate training. We observe that embedding accesses are heavily skewed, with almost 1% of embeddings represent more than 92% of total accesses. Further, we observe that during training we can lookahead at future batches to determine exactly which embeddings will be needed at what iteration in the future. Based on these insight, we propose Bagpipe, a system for training deep recommendation models that uses caching and prefetching to overlap remote embedding accesses with the computation. We designed an Oracle Cacher, a new system component which uses our lookahead algorithm to generate optimal cache update decisions and provide strong consistency guarantees. Our experiments using three datasets and two models shows that our approach provides a speed up of up to 6.2x compared to state of the art baselines, while providing the same convergence and reproducibility guarantees as synchronous training.

1 Introduction

Recommendation models are widely deployed in enterprises to personalize and improve user experience. Applications that use recommendations range from personalized web search results [37] to friend recommendations in social networks [28, 9] and product recommendations on e-commerce websites [24]. Further, recommendation algorithms are also known to have significant impact on the revenues of organizations, *e.g.*, 35 percent of consumers purchases on Amazon and 75 percent of what people watch on Netflix come from product recommendations based on such algorithms [29]. With growing data sizes [2] and the use of recommendation in increasingly sophisticated tasks [13, 22], recent trends have seen the adoption of new deep-learning based recommendation models [6, 35]. These models have become one of the largest ML workloads with companies like Facebook reporting that more than 50% of all training cycles [2] and more than 70% of inference cycles [10] are used for deep learning based recommendation models (DLRM).

The structure of recommendation models differs significantly when compared to CNNs or DNNs introducing new challenges to efficiently scale training. This is because recommendation models contain two types of model parameters: embedding tables that store vector representation of categorical features and neural networks (bottom and top) that consist of multi-layer perceptrons (MLP) for numeric features. If we consider a click-through-rate (CTR) prediction model, given a batch of training examples (user clicks), in the forward pass we first look up the relevant embeddings for categorical features of the input. We note that the embedding lookup is *sparse*; for instance if the user location is New York, we only need to fetch the embeddings corresponding to that location from the embedding table which contains all the major cities. The numerical features are processed by a *dense* MLP and the representations are then combined to form a prediction as shown in Figure 1. Similar to existing DNNs, in the backward pass the embeddings and the MLP parameters are updated based on gradients calculated.

The main challenge in scaling the training of DLRM models arises from the extremely large, memory-intensive embedding tables. Table 1 shows the size of embedding tables for three open source datasets. In production systems embedding tables up to terabytes in size [46, 10] are common. This motivates the use of a hybrid parallelization approach in prior work [30, 2] where the dense MLP layers are *replicated* across GPUs in training workers, while embedding tables are *partitioned* and stored on the CPU memory of workers, leading to a design where model parallelism is used for embedding layers and data parallelism is used for dense MLP layers.

Despite using hybrid parallelism, we find that existing approaches to DLRM training suffer from low compute resource (GPU) utilization and data access bottlenecks. In Figure 2, our profiling on a 8 GPU cluster with the Criteo dataset (details in Section 5) shows that on each iteration, only 8.5% of the GPU time is spent in forward / backward computations. Embedding fetch, and write back of updated embeddings takes around 75% of the overall iteration time. This motivates us to ask: *can we design a system for training recommendation models that can alleviate embedding access bottlenecks?*

Our key insight in this work is that access to embeddings have specific structure and patterns that can be used to accelerate training. First, as shown in Figure 4 our analysis across three datasets indicates significant *skew* in embedding accesses, *e.g.*, for the Kaggle (Criteo) dataset we observed that 90% of accesses are for just 0.1% of the embeddings. While this might indicate that we can just *cache* popular embeddings in GPU memory [3], we find that to be insufficient. We find that each training batch also requires a number of embeddings that are not present in the cache. In Figure 6 if we calculate the proportion of embeddings read from the cache to the total number of embeddings accessed, we observe that for a batch size of 16,384 with the same Criteo Kaggle dataset and having the 0.1% most popular embeddings in cache, only 15% of the embedding accesses will be from the cache. This indicates that the long-tail of embeddings dominates accesses. The above observation leads us to our second key insight that when performing offline training of ML models, we can *lookahead* of the current batch, and inspect future batches. Using this insight we can determine exactly which embeddings will be needed at what iteration in the future. That is, we can *prefetch* embeddings based on when they will be used and additionally cache them in GPU memory if they are going to be reused in the near future. Prefetching helps overlap embedding fetches for future batches with compute of the current batch, effectively hiding the latency of embedding fetch.

Based on these insights we build BAGPIPE, a system for efficient distributed training of large scale recommendation models. Central to our design is an *Oracle Cacher* (Section 3.2), a new service that looks beyond the current batch, and determines which embeddings need to be pre-fetched and/or cached. We also develop a *dynamic cache* (Section 3.3) that is located on each training worker and workers overlap cache additions and evictions with model training. We provide a strong consistency guarantee that training in BAGPIPE matches synchronous training used in existing DLRM training frameworks and show that despite fetching embeddings out of order we can ensure consistent access to embeddings across batches. Further, we compose our new services in a disaggregated training architecture that separates data loading from training and show that this alleviates data loading bottlenecks while allowing independent scaling of various training components based on the model and dataset requirements. Finally, we also show that our training setup allows the possibility of overlapping almost all the communication and cache management with the compute of a training loop therefore hide almost all the communication and additional overheads of cache management.

We evaluate BAGPIPE using three datasets, Criteo Kaggle [20], Avazu [16] and Criteo Terabyte [21], and two different models, Facebook’s DLRM [32] and Google’s [6] Wide&Deep. We scale up our training to model sizes of 14.2 billion parameters and using up to 16 GPUs. Overall we find that BAGPIPE can improve iteration time by $6.2\times$ compared to DLRM [35] and $1.8\times$ compared with static caching in FAE. We also show that our proposed Oracle Cacher based design can fully overlap embedding fetch with model training, thereby reducing network accesses on the critical path, while imposing low overheads.

2 Background & Motivation

We begin by providing background on recommendation model training and motivate the need for a new system that optimizes data movement.

Table 1: **Size of Embedding Tables:** We show size of embedding tables for three open source datasets. We assume the embedding dimension to be 48

Dataset	Embedding Table Size	Datapoints
Criteo Kaggle	6 GB	39.2Million
Avazu	1.7 GB	40.4 Million
Criteo Terabyte	157 GB	4.37 Billion

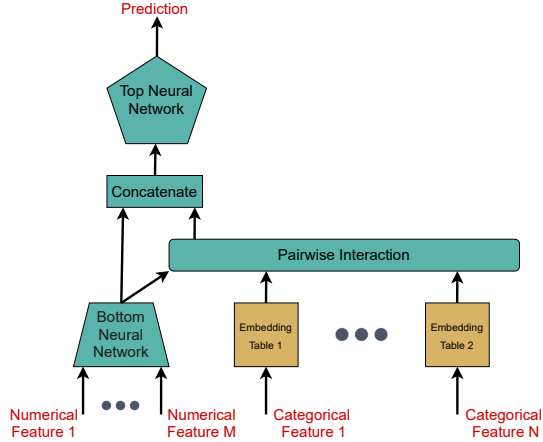


Figure 1: **Architecture of a recommendation model:** Above is a schematic of a typical deep learning based recommendation model(DLRM).

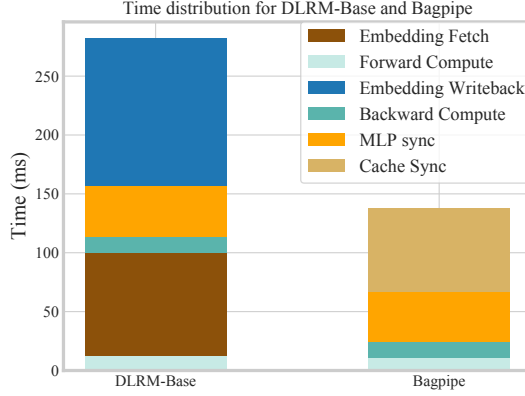


Figure 2: **Time Distribution in training:** We plot the average time spent in various stages. The training was performed on 8 *p3.2xlarge* instances on Kaggle Criteo dataset. The above time excludes data loading time for a fair comparison.

2.1 Deep Learning Recommendation Models

Recommendation models are widely used in industry to power several large scale internet services. Recent work has proposed using deep learning to improve accuracy of recommendations [32, 6, 17]. All deep recommendation models consists of two types of components (i) a memory intensive embedding layer which stores a mapping between the categorical features and their numerical representations (ii) a compute intensive neural network based modeling layer used for modelling interactions between numerical features and vector representations of categorical features. Across models the structure of embedding tables typically remain the same. The number of rows (elements in the table) usually depend on the dataset, *i.e.*, the number of categories, while machine learning engineers vary the dimension of embedding *i.e.*, the size of the vector to represent a categorical feature. Common dimensions of embeddings are 16, 32, 48 and 64 with embeddings sometimes being as large as 384 [30]. However, the number of elements in an embedding table vary widely and can be as small as 3 elements or as big as a few billion elements depending on the dataset [46, 10]. Neural network layers have more diversity and the type of neural network usually depends on the modelling task at hand. DLRM [32], a recommendation model from Facebook used for predicting click through rates, uses fully connected neural networks for both bottom and top neural network, while TBSM [17], a model used for predicting a user’s next interaction based on previous interactions uses a modified version of multi-head attention as the top neural network while still using a fully connected neural network for bottom neural network. The forward pass of training involves looking up embedding vectors corresponding to the data items, this stage is shared by all deep learning based recommendation models [42, 44, 43, 41, 7] as embeddings are necessary to handle categorical features such as location, interaction type, product type, gender to name a few.

In this paper, our focus is to reduce data access overheads that arise from performing embedding lookups and speedup training of all the recommendation models which use embedding tables.

2.2 Training Recommendation models

Next we discuss the system setup used for training recommendation Models.

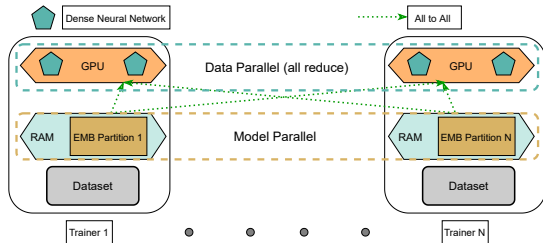


Figure 3: **Common distributed DLRM training setup:** The above figure represents a typical DLRM training setup. The dense NN layers are replicated across GPUs while the embedding layers are partitioned and kept in the main memory.

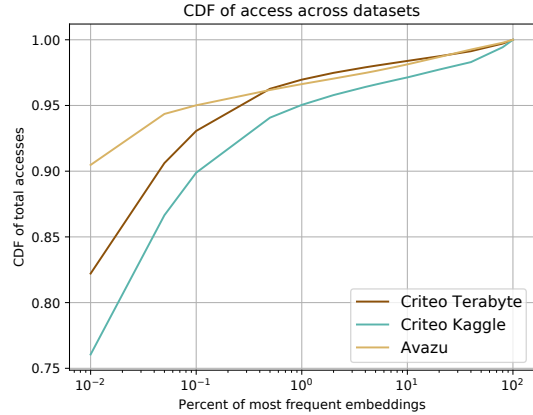


Figure 4: **CDF of embedding accesses:** The embedding access pattern is heavily skewed, with just top 0.1% of the embeddings responsible for more than 90% of total accesses.

Training Setup. Recommendation models are extremely large and are currently among the largest ML models used in enterprises. Recently Facebook released a 12 Trillion parameter recommendation model [30]; in comparison GPT-2 is 175 Billion parameters. However, more than 99% of parameters in these models are for embedding tables which have sparse access patterns. This extremely large model size combined with the sparse access pattern introduces a number of new challenges in distributed training. Figure 1 shows a schematic of a deep learning based recommendation model. In a typical DLRM training, neural network (NN) parameters are stored on the GPUs and are replicated. The dense NN parameters are trained in data-parallel fashion and gradients are synchronised using the all-reduce communication collective. However, embedding tables are extremely large to hold in single GPU memory and often can not even fit into CPU memory of a single worker. Therefore, embedding tables are typically partitioned across nodes and stored in CPU memory, thus being trained in a model-parallel fashion. The embeddings are fetched using the all-to-all collective [1]. Figure 3 gives an overview of the existing training setup. In our experiments we observe that almost 75% of the time is spent in embedding lookups and write-backs, when performing training on 8 *p3.xlarge* instances.

Beyond spending a large proportion of training time in embedding lookups, the existing setup couples storage and compute resources used for training. For example, if the embedding tables for a model are extremely large but the compute requirements are very small, one still has to use large number of machines with GPUs to store the embedding tables. This often leads to sub-optimal use of compute resources.

Synchronous vs. Asynchronous Training. To speed up training of DLRMs and improve resource utilization several prior works [14, 2, 11] have proposed using asynchronous training methods. With asynchronous training the embedding fetch can happen in parallel. However, similar to other ML models, recent works [14, 30] have observed that using asynchrony can lead to degradation in accuracy for recommendation models. This degradation in accuracy is unacceptable to large enterprises as it often directly leads to loss in revenue [30]. Another reason data scientists avoid asynchronous training is the lack of reproducibility, which is necessary to reason about and compare different model versions. Therefore, in this work we focus on improving the performance of *synchronous distributed training*.

2.3 Embedding Access Patterns

Next we describe some of our insights relating to embedding access patterns observed in recommendation model training.

Skew in embedding accesses. When profiling embedding accesses across three datasets (details in Section 5.1), similar to prior work [3], we find that embedding access pattern shows a large amount of skew. As shown in Figure 4 we observe that almost 90% of embedding accesses come from just 0.1% of the embeddings.

This is because, for example, in online shopping settings, some item IDs are accessed far more frequently because the corresponding items are more popular. This naturally indicates that caching *hot* embeddings can reduce lookups significantly. Thus, when a training example needs a popular embedding, it can directly use it from the local cache; else *cold* embeddings need to be fetched from the corresponding embedding server. This leads to the question of how to detect which embeddings are hot enough to cache them in local GPU memory.

Caching frequently accessed embeddings has been studied by [3] where they propose a Frequently Access Embedding (FAE) framework. The authors in [3] pre-process a sample of the dataset to determine popular embeddings and then cache these embeddings in GPU memory. However, we observe that just static caching is not enough: we next discuss how changes in embedding popularity and mini-batch construction lead to challenges when using static caching.

Popularity of embeddings change over time. We measured the change in popularity over time across three datasets (Criteo, Alibaba and Avazu) using the following method: we first chose a fixed fraction of the most popular embeddings in the first day (*e.g.*, top 1% most popular embeddings), and then measured what percentage of accesses consist of those embeddings in the later days. Figure 5 shows that in all three datasets, using a fixed set of popular embeddings from the first day (day 0) would lead to worse cache hit ratio on the following days, *e.g.*, in the case of the Avazu, if we chose the top 0.05% of the most popular embeddings to be in the cache, the percentage of accesses to those embeddings changes from around 91% on the first day to around 82% on day 9. This shows that it is not possible to use a fixed set of popular embeddings and thus existing approaches which focus on static caching [3] will require additional steps for regular update of popular embeddings.

Long-tail of accesses limits benefits from caching. Further, we find that only caching a set of popular embeddings is not enough when training with large batch sizes. When the batch size increases, we observe that a large number of embeddings are still required to be fetched from outside the cache thereby affecting training throughput. Figure 6 shows the distribution of embeddings fetched from the cache as we increase the batch size. Most notably, we see that as batch size increases the ratio of embeddings fetched from the cache to the total number of unique embeddings needed in a batch keeps decreasing drastically, *e.g.*, for a batch size of 16,384 only around 10% of the total unique embeddings required are fetched from the cache. To solve this issue prior work in FAE [3] partitions the examples into hot and cold batches. Hot batches consist of examples which access all their embeddings from the cache, while cold batches have examples which need embeddings not present in the cache. Then for some duration they train using hot batches and during other intervals training is performed on cold batches. However, this impacts the statistical efficiency as training continuously with hot batches and then continuously with cold batches changes the order of the training examples and thus affects convergence [3]. To mitigate the loss in accuracy, one needs to frequently switch between hot and cold embeddings which requires synchronizing caches with the embedding tables stored in main memory. This synchronization in the distributed setup (more than one node) is expensive. Moreover, it is not always possible to create hot batches that only access cached embeddings. This is because some models [26, 22] use features like Unique User ID (UUID) and Unique Session ID [39, 38, 40] as features. These features are unlikely to be repeated a significant number of times in the dataset and thus every example requires access to at least one cold embedding.

In summary, embedding access pattern across different dataset presents an opportunity to enable data access optimizations. However, existing systems that rely on static caching, require pre-processing before training and can affect statistical efficiency. Based on these motivation we next seek to design a new system that can take advantage of the skew in embedding access pattern while handling popularity changes and seamlessly integrating with user code without affecting accuracy.

3 BagPipe

Next we discuss BAGPIPE, a system for large-scale training of recommendation models.

3.1 Design Overview

To enable large scale recommendation model training, BAGPIPE introduces three major design contributions.

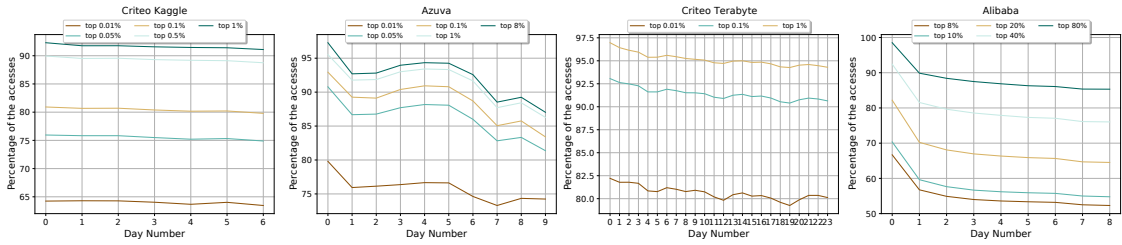


Figure 5: **Popularity change across days:** For the above experiment we show the embedding popularity changes in the temporal domain. In the above figure we choose the popular embeddings on day zero and show how the number of accesses provided by the popular embeddings chosen on day 0 change over consecutive days. For some datasets we observed that the number of accesses provided by the cached popular embeddings decrease by as much as 20%. This shows that we will have to compute our popular embeddings everyday if we want a high cache hit rate.

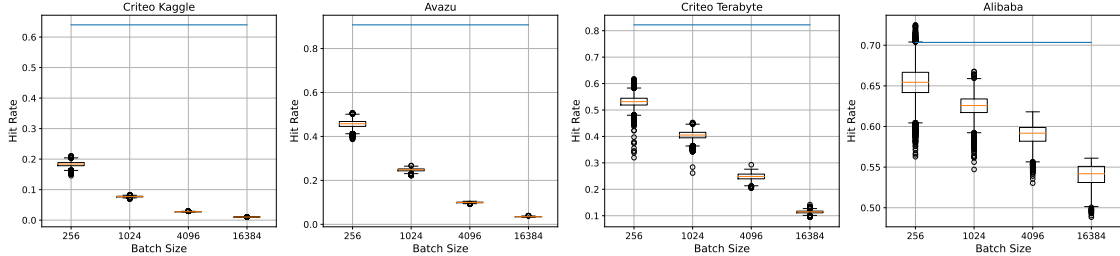


Figure 6: **Distribution of unique embeddings accessed from the cache:** The ratio of unique embeddings accessed from the cache decreases as we increase the batch size. The blue line represents the expected hit rate when storing the most frequently accessed 0.1% embeddings.

First, we design a new embedding caching mechanism that can exploit the skew in access patterns while handling changes in popularity and long tail accesses. To do this we introduce a dynamic *oracular* cache which is designed to *lookahead* at future training batches to determine cache additions and evictions. Detailed design and analysis of our caching mechanism can be found in Section 3.2.

Second, in contrast to existing training setups (Figure 3) BAGPIPE uses a dis-aggregated architecture which can independently scale embedding table partitions and trainers depending on the properties of recommendation model being trained. Figure 7 provides an overview of BAGPIPE system design. Details of all the components and design decisions pertaining to each component are provided in Section 3.3.

Third, BAGPIPE is designed to pipeline or overlap communication and cache management with the compute required for model training. This allows maximum utilization of compute resources. Section 3.4 provides details on how BAGPIPE has the potential to eliminate almost all the communication from the critical path.

3.2 Caching in BagPipe

As discussed in Section 2.2 and shown in Figure 6 static caching is not able to provide promised speedups. In BAGPIPE we explore creating a dynamic cache which can add and evict elements dynamically by analyzing batches that will be trained in the future. For this purpose we introduce the concept of Lookahead value(\mathcal{L}) which determines the number of batches ahead of the current batch we are going to look at to make decision about caching. For example, if the current batch is x , we look at all batches from x to $x+\mathcal{L}$, to determine which elements should be cached.

Next we introduce various components which enable caching in BAGPIPE. First we present how caches are maintained in a single GPU setting. Then we discuss how to extend this to a distributed setting.

Deciding what to cache and for how long. One of the most important decision when performing caching is deciding what to cache. To decide what to cache BAGPIPE relies on one key insight, *in offline batch training the batches and their contents are predictable*, i.e., we can look beyond current batch and exactly find out which embeddings will be accessed by future batches. This insight enables BAGPIPE to

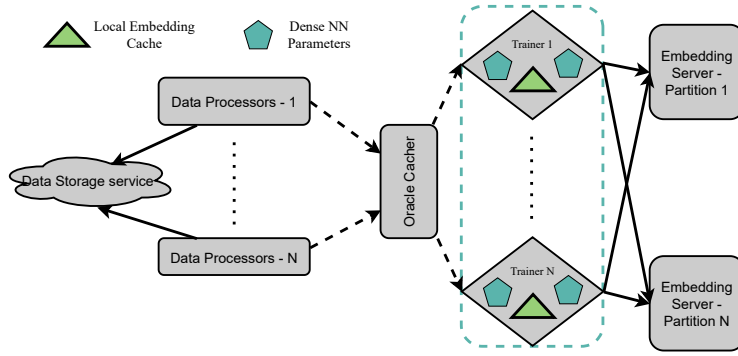


Figure 7: **BagPipe setup:** All the components of BAGPIPE can be individually scaled. The dashed arrows signify async RPCs while solid ones signify sync RPCs. The Trainers are synchronized using Allreduce primitives.

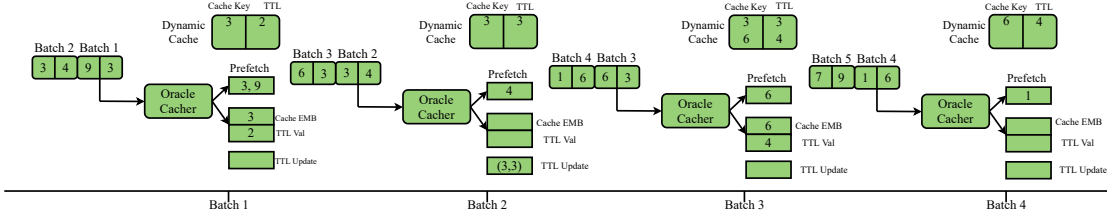


Figure 8: **Original DLRM:** The above figure shows an illustration at different batch steps how lookahead algorithm functions. In the above example the lookahead value is 2 and the batch size is also 2.

look-ahead beyond the current batch and create a perfect or an *oracular* cache [5].

For deciding what to cache and what to evict we build an extremely low overhead (benchmark in Section 5.5) lookahead algorithm (Algorithm 1) that also ensures consistent access to embeddings. To design the lookahead routine, we first introduce a parameter called *lookahead value* (\mathcal{L}). \mathcal{L} signifies the number of batches ahead of the current batch we are going to analyse to determine what to cache. The lookahead algorithm takes three inputs: the current batch, future batches (as many required for lookahead) and current state of the dynamic cache. For example, if the lookahead routine is processing batch number x and lookahead value is set to y , the lookahead routine will need the current batch x and next y batches of training data.

The lookahead algorithm outputs three pieces of information. First, for a given batch it generates the list of embeddings which will not be found in the cache on the trainer GPUs. This allows us to *prefetch* this list of embeddings early and move those elements to the cache, before the current training batch is chosen for training. Prefetching allows BAGPIPE to hide the data access latency for the long tail of embeddings that are not frequently accessed. Second, the lookahead algorithm determines *which embeddings from the current batch will be used in future batches*. Any embeddings from the current batch that will be used by any of the future batches within the *lookahead* window will be marked for caching, so they can be accessed from the GPU memory in future. Third, the lookahead algorithm determines the time-to-live (TTL) for each element in the cache. Next we provide details of our lookahead algorithm.

Lookahead Algorithm Our lookahead algorithm is shown in Algorithm 1. The algorithm takes in the preset lookahead value (\mathcal{L}) as an argument and dynamically keeps a window of batches of that size. The window is maintained as a queue, where the next batch to be processed is in the front of the queue. As shown in Line 5-12, when the window size is smaller than the look-ahead value (at the beginning of the training or after a batch is processed), the algorithm extends the window by reading new batches from the data loader. Meanwhile, it keeps the last occurrence of each embedding in this window. After ensuring that the window size is equal to \mathcal{L} (or there are no more batches to process), the algorithm starts to process the first batch in the window, as shown in Line 15-27. For each embedding, it adds a request for updating the TTL as the last occurrence of this embedding, and then it adds a pre-fetch request if this embedding is not in cache. For an embedding e , suppose the last iteration it appears in (including the current one) is x . *InCache* has e if and only if it has occurrence number y such that $y - x < \mathcal{L}$. We maintain this invariant in Line 21 and 24. This guarantees that when the iteration y starts, the trainer will only pre-fetch e when e

did not appear in any batch in the range of $[y - \mathcal{L}, y)$.

In Line 25, we also safely erase embedding e from *LatestTracker* if e is not in the cache to ensure that the memory complexity is linear to the number of embeddings that appear in the window. This is an update to the cache status which is maintained locally.

We next take a look at an example of the lookahead algorithm in action in Figure 8. We set the lookahead value (\mathcal{L}) as 2. The figure shows a window of batches being processed by the lookahead algorithm and producing cache update requests.

The local embedding cache in Figure 8 keeps track of what is in the *InCache* variable in the algorithm.

- **Batch 1** Embedding 3 and 9 are in the batch. For both embedding 3 and 9, we will launch prefetches. However, for embedding 3, we see that it is accessed again, and last occurrence in the window is at Batch 2, so we decide to cache it with the TTL set to 2.
- **Batch 2** For embedding 3, we see the last occurrence in the window is in Batch 3 and it is in the cache, so we will send a TTL request with value 3. We will not launch a prefetch for 3 because 3 is already in the cache, while we will prefetch 4 since it is not in the cache.
- **Batch 3** For embedding 3, we do not see any future occurrence in the window, so we will not send any updates for 3. For embedding 6, we decide to cache it with a TTL of 4 because it appears to be used in Batch 4. Embedding 3 will be deleted from *InCache* after this batch.
- **Batch 4** For this iteration, we will prefetch 1 since it is not in the cache. We do not send any TTL updates for 6 as it is absent in future batches. It will be deleted from *InCache* after this batch.

Next we look at how we extend our cache to a distributed setup.

Dynamic and Replicated Cache. For creating a cache in distributed setting, we design a dynamic cache that resides on each worker to be *replicated*. We chose a replicated cache primarily for two reasons. First, from our experiments we determined that even for extremely large \mathcal{L} values we barely need a gigabyte of GPU memory for the cache (Figure 16a). A gigabyte of memory is easily available on modern GPUs even for the most compute intensive DLRMs. With a local batch size of 2048 we only need 1.8GB of memory out of 16 GB on a V100 for model training, leaving almost 14 GB of DRAM free. Secondly, a non-replicated cache will require additional control logic to provide load balancing and synchronization, which can make our training batch dispatch quite slow. Therefore, we chose to use a replicated cache. The main overhead in using a replicated cache is that its contents have to be synchronized at the end of every training iteration. In Section 3.4 we discuss how we are able to move a significant portion of synchronization out of the critical path and overlap it with forward and backward pass.

Guaranteeing Consistency. Our formulation of what to cache and when to prefetch, provides a subtle but an extremely important guarantee that allows us to scale while matching the execution of synchronous training. The key consistency goal in our design is to ensure that workers do not pre-fetch an embedding from the embedding servers while it has updates in cache that have not been written back. To achieve this goal, we derive an invariant that the lookahead algorithm maintains. When lookahead algorithm is processing batch number x , either an embedding needed by the batch with its most updated value will be available in the cache when the batch is processed or no preceding batch in the lookahead range (any batch number in $[x - \mathcal{L}, x)$) is going to update that specific embedding. To emphasize this again but in a slightly different manner, if an embedding was needed by a batch in batch number in range $[x - \mathcal{L}, x)$ it will be in the cache; if it is not in the cache it means no batch in range of $[x - \mathcal{L}, x)$ has updated it. Therefore, as long as the prefetch request is issued after updates from training batch number $x - \mathcal{L}$ have been written back, we can safely prefetch embeddings without being concerned about staleness. This specific condition guarantees that despite fetching embeddings out of order we will still see the same results as synchronous training.

3.3 BagPipe Design

As shown in Figure 3 and discussed in Section 2.2 the existing distributed training setup based on the implementation by Facebook [35] couples storage and compute resources, *i.e.*, we cannot scale the number of embedding table partitions without increasing the number of trainers. We believe *disaggregation* is extremely


```

Input: LookAheadValue
1 BatchQueue = Queue();
2 LatestTracker = Dictionary();
3 InCache = Set();
4 while BatchQueue.size() > 0 do
5   while hasNextBatch() and BatchQueue.size() < LookAheadValue do
6     Batch = getNextBatch();
7     IterationNumber = Batch.IterationNum;
8     for EmbID ∈ Batch.UniqueEmbeddings() do
9       LatestTracker[EmbID] = IterationNumber ;
10      BatchQueue.pushBack(Batch);
11    end
12  end
13  TTLUpdateRequests = {};
14  CacheFetchRequests = {};
15  CurrentBatch = BatchQueue.popFront();
16  for EmbID ∈ CurrentBatch.UniqueEmbeddings() do
17    TTL = LatestTracker[EmbID];
18    TTLUpdateRequests.append((EmbID, TTL));
19    if EmbID is not in InCache then
20      CacheFetchRequests.append(EmbID);
21      InCache.insert(EmbID);
22    end
23    if TTL = CurrentBatch.number then
24      InCache.erase(EmbID);
25      LatestTracker.erase(EmbID);
26    end
27  end
28  SendToTrainers(TTLUpdateRequests);
29  SendToTrainers(CacheFetchRequests);
30 end

```

Algorithm 1: Lookahead Algorithm

important for better resource utilization and scalability [8, 4]. For example, when embedding tables are extremely large but the dense neural network parameters are small and do not require large amounts of compute, an optimal configuration would be to use more servers for embedding tables but have fewer trainers.

We design a disaggregated architecture which can independently scale different components of training using four major components: (i) Data Processors (ii) Oracle Cacher (iii) Distributed Trainer (iv) Embedding Servers. Figure 7 shows a schematic of our system design. All the components communicate with each other over RPC (we use a mix of asynchronous and synchronous RPCs). For synchronizing the dense parameters and updates in the dynamic local cache we use the MPI AllReduce primitive. We next provide details of each of our system component.

Data Processor. Prior work [47, 30] has shown that data processing for recommendation models is very compute intensive. Data processing if performed on the same node on which training is performed, can reduce the throughput of recommendation model training by as much as 56% [47]. Inspired by the design proposed in [47] we offload the data processing from the training nodes to remote nodes which are exclusively used for data processing. Depending on throughput requirements the users can scale-up or scale-down the nodes used for data processing. Since the communication is over RPC, the users of BAGPIPE can also choose to pack data pre-processors with other functionalities as well.

Oracle Cacher. Oracle Cacher is one of the main components of BAGPIPE. Oracle Cacher is where we implement the look-ahead routine discussed in Algorithm 1. Oracle Cacher is a centralized service which inspects all the processed training batches and determines the cache contents. Using the lookahead algorithm(1), Oracle Cacher decides which elements to prefetch for the current batch, which elements to cache from the current batch and if the lease (TTL) of an element existing in the cache needs to be updated.

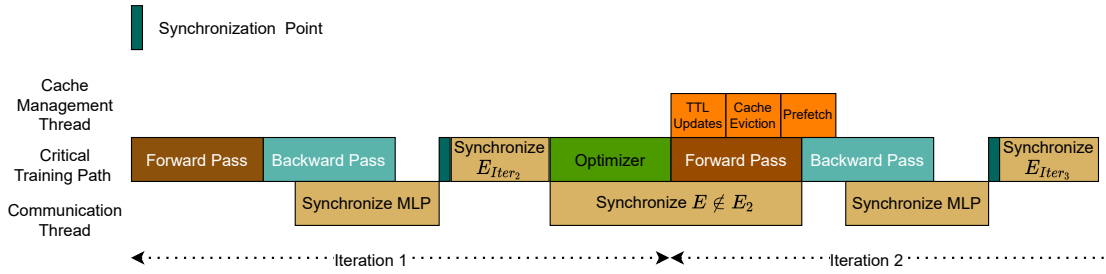


Figure 9: **A schematic of how overlapping various operations work:** The above figure shows an illustration of how BAGPIPE manages to minimize the communication and cache management on the critical path. We show that how BAGPIPE only synchronizes those embeddings on the critical path which are going to be used by the next iteration. For example - In iteration we only synchronize embeddings needed in iteration 2 (E_{iter_2}). Rest of the embeddings ($E \notin E_{iter_2}$) are synchronized off the critical path. Further before each synchronization of embeddings we have a *Synchronization Point* where we check all off-the-critical synchronization have finished before launching other communications.

Oracle Cacher is also responsible for routing batches of training data to the workers. Oracle Cacher sends the prefetch requests, training data as well as the cache information using async RPC calls to the trainers. An important point to note is that the cache changes for a certain iteration x does not happen when the oracle cacher generates the requests. Those requests are sent to the trainers with the iteration number to apply them at. The requests are then applied by the trainer at an appropriate time so as to maintain consistency. To reiterate, state changes to caches is performed by the trainers, the Oracle Cacher just generates what the trainers are supposed to do and at what iteration. This transfer of control to trainers and using iteration number for coordinating when to perform an action minimizes the co-ordination required between Oracle Cacher and training nodes, while providing consistency guarantees.

Trainer. Trainers are GPU machines, which hold the dense neural network portion of recommendation model in the GPU memory. Trainers also consist of the dynamic cache where the embeddings needed by future batches are stored. The trainers perform forward and backward passes in a synchronous fashion, *i.e.*, at the end of each batch the gradients of the dense neural networks are synchronized. Apart from training the dense neural network, trainers perform two other critical operations. One is prefetching the embeddings based on requests sent by Oracle Cacher and second is cache maintenance. Cache maintenance includes addition and eviction of embeddings, and updates to the TTL values. The trainers perform prefetching by sending asynchronous requests to Embedding Server. As discussed previously (Section 3.2), our lookahead provides consistency as long as prefetch requests for embeddings needed by a batch x are dispatched, only after the training and updates for batch $x - \mathcal{L}$ have been propagated to the embedding servers, *e.g.*, if \mathcal{L} is 40 and x is 100 then as long as prefetch request for remote embeddings (embeddings not in local cache) needed by batch number 100 (x) are made after processing batch number 60 ($x - \mathcal{L}$) our formulation will provide consistency guarantees similar to synchronous training. For cache evictions all elements whose TTL value is less than currently processed iteration number are evicted.

Embedding Server. Embedding servers store all the embedding tables and act as a sharded parameter server. They handle the prefetch and update requests from the trainer. Typically an Embedding Server runs on a high memory machine due to the large size of embedding tables. We use the Embedding Bag abstraction [34] provided by PyTorch to store the embeddings. The Embedding Server exposes two RPC functions, one to fetch embeddings and the other to receive updated embeddings from the trainers and correspondingly update the local version based on the new values.

3.4 Overlapping cache management and communication with computation

BAGPIPE is designed to minimize any additional compute and communication on the critical path of training. To achieve this we use the idea of overlapping all such operations with computation of forward and backward pass that take place on the trainers. Figure 9 shows a schematic of how BAGPIPE can potentially hide most of the extra overhead by overlapping the prefetch and cache maintenance actions described before with the compute required for model training. We next describe optimizations we design to achieve this.

Overlapping cache management with training. Cache management in BAGPIPE consists of primarily three operations. First, we need to update the TTL of elements in the cache based on values sent by Oracle Cacher. Second, we need to evict the elements which have TTL less than current iteration number and upon eviction we need to update the latest value on the Embedding Server by making a RPC call. Third, we need to launch prefetch requests sent by Oracle Cacher, for any iteration number which is needed within next \mathcal{L} batches, *i.e.*, if the current iteration number is x we should launch prefetch requests for an iteration number $(x, x + \mathcal{L}]$.

We perform, all cache management operations in a separate thread thus not affecting the training process. We would like to point out that our caching data structure can operate completely lock free, because in our lookahead formulation in Oracle Cacher, it is guaranteed that the training thread and cache maintenance thread will operate on completely separate indices of the dynamic cache. Further, our main training thread only sends a signal to the cache management thread indicating which iteration number has finished and no other additional synchronization is needed. This setup ensures that caches have minimal overhead.

Overlapping Cache Synchronization. Replicated Caches need to be synchronized and this synchronization which happens after the forward/backward compute is on the critical path of training. We perform two additional optimizations to improve the performance of synchronization. First, instead of synchronizing the whole cache we only synchronize gradients of the elements which have, been updated in the current iteration. Next, we perform an additional optimization in which we initially only synchronize the elements which will be required in the next iteration. We schedule rest of the elements to be synchronized in the background. Thus, only a very small portion of the cache entries are synchronized on the critical path. From our experiments on Kaggle criteo dataset with 8 *p3.2xlarge* and batch size of 16,384, these optimizations lead to an average 3,471 entries out of 14,184 entries that need to be synchronized on critical path. Thus, our optimizations reduce the communication on critical path by almost 75%, and help us overlap a large portion of cache synchronization with compute. We evaluate the effect of these optimizations in Section 5.5

3.5 Discussion

Next we qualitatively discuss some benefits and limitations of BAGPIPE’s design.

Generalizing across skew patterns. Unlike prior work [3], BAGPIPE’s optimizations will hold even if embedding access skew or popularity changes drastically over time. The primary reason for this is that BAGPIPE does not only rely on caching of hot embedding to provide speedups. It is also able to handle cold embeddings by using pre-fetching. So if there exists datasets which do not display high degree of skewness, BAGPIPE will just have to prefetch more but it should still be able to provide gains in throughput.

Transparency to the user. Unlike prior work [46, 3] BAGPIPE is completely transparent to the user. It produces the exact same result which a user would have got if they ran vanilla synchronous training. Our prefetching and caching guarantees are similar in spirit to out of order executions performed in computer architecture [15].

Memory pressure. Since BAGPIPE stores the local embedding caches in the accelerator memory it can lead to extra memory pressure on accelerator memory. However, we observe that the memory requirement of dense NN parameters is quite small, *i.e.*, at batch size of 2048 dense NN parameters only consumed 1.8 GB of accelerator memory out of the 16 GB available on a V100 memory. This leaves ample space for caching embeddings. We also allow users to configure a maximum cache size and adaptively adjust the lookahead values to make sure the cache size remains bounded.(Section 3.6)

Performance on slow networks. If embedding fetch is extremely slow (say due to a slow network connection), BAGPIPE can not guarantee that embedding fetch for a batch from the remote embedding server will complete before the training begins. Hence it will have to block. This is because BAGPIPE relies on overlapping embedding fetch with computation of dense parameters. However, if the fetch is slower than compute we will start observing the latency of embedding fetch in the train loop. In the data-center setting we observe that BAGPIPE is able to completely overlap the training time with embedding fetch and hides the fetch latency. However, even in the case embedding fetch is slow, BAGPIPE is expected to perform significantly better than baseline because of overall reduction in number of embedding fetches due to caching.

Applicability in online training. BAGPIPE’s optimizations are only applicable in the offline training regime. This is because BAGPIPE relies on the ability to look at future batches and build a cache which is guaranteed to provide a hit. However, in case of online training where training examples arrive sporadically

BAGPIPE will not be able to do so.

Scalability of Oracle Cacher. A limitation in our design is that Oracle Cacher is not horizontally scalable. However, the overhead of Oracle Cacher is extremely small (less than 70ms) even for extremely large batch sizes and lookahead values. Thus we believe Oracle Cacher will still be able to support training at extremely large scale. In Section 5.5 we study the scalability of Oracle Cacher.

3.6 Automatically Calculating Lookahead

BAGPIPE requires two configuration parameters: one is maximum cache size and the other is lookahead value. Providing the maximum cache size is mandatory and if the user does not provide a lookahead value it is automatically computed by BAGPIPE. Users can determine maximum cache size by computing how much free memory is available on the GPU after allocating space for the dense neural network parameters. If the lookahead value is not provided, at the beginning, BAGPIPE keeps prefetching until it detects the cache is full. On detecting that the cache is full, BAGPIPE selects the current number of batches prefetched so far as the lookahead value. Further, BAGPIPE can also handle scenarios where the configuration variables are incompatible. Since Oracle Cacher always has a consistent view of the cache, it can determine when the cache will be full. If Oracle Cacher observes that cache is going to be full it reduces the lookahead value by half. We present results from a sensitivity analysis in Section 5.5.

4 Implementation

We have implemented all the modules in around ≈ 3000 lines of Python. Users can use the PyTorch API for creating deep learning based recommendation models. Further we also rely on Torch RPC framework for communicating with different components of our architecture. Except for the communication between the Trainers and Embedding Server we use asynchronous RPC calls for better scalability. For synchronizing the dense parameters we use collective communication primitives from the PyTorch distributed data parallel module.

We next describe some additional optimizations implemented in BAGPIPE.

RPC batching. As described previously, after evicting an embedding from the cache we send an embedding update request to Embedding Server. The embedding update request contains the latest value of the embedding. We perform this in a separate thread once we have processed the training example, *i.e.*, once the trainer has trained on batch number x , it signals the background thread of batch x 's completion. The cache maintenance thread evicts the elements which have TTL less than or equal to completed batch numbers, and sends the updated value to the Embedding Server. We observed that making the update RPC call at every batch leads to high overhead on Embedding Server and limits the throughput. To avoid this we batch the RPC calls and set the batch size as a fraction of our lookahead value. For example, *e.g.*, if our RPC batch proportion is 0.25 and the lookahead value is 200, then cache eviction is performed at every 50th iteration. Using an extremely high RPC batch proportion delays eviction, which can in turn block prefetch requests. This is because, to guarantee consistency, we cannot prefetch until eviction is complete.

Eviction Load Balancing. Since all our caches are replicated and synchronized, the update RPC to Embedding Server can be sent by any of the trainers. Instead of repeatedly sending update RPCs from one specific trainer we switch to a different trainer for each successive request. For examples, if there are 4 trainers, and the previous eviction request was sent by trainer number 4, then the next eviction request will be sent by trainer number 1. We note that all the workers perform eviction on their local caches and this optimization only relates to which worker calls the update RPCs. With this optimization the network load is evenly balanced during training.

5 Evaluation

5.1 Experimental Setup

Models and Datasets. We evaluate the performance of BAGPIPE across three different datasets and two models. For datasets we use Kaggle Criteo [20], Avazu [16] and Criteo Terabyte dataset [21]. For models we use Facebook's DLRM [32] and Wide and Deep [6] which was proposed by Google. Table 2 describes the datasets showing total number of datapoints and the number of categorical and numerical features associated

Table 2: Dataset and Model Description

Datasets	Training Input			Neural Network		Embedding Tables	
	Datapoints	Categorical Features	Numerical Features	Bottom MLP	Top MLP	Number of Embeddings	Embedding Dimension
Kaggle Criteo	39.2 Million	26	13	13-512-256-64-48	1024-1024-512-256-1	33.76 Million	48
Avazu	40.4 Million	21	1	1-512-256-64-48	1024-1024-512-256-1	9.4 Million	48
Terabyte	4.37 Billion	26	13	13-512-256-64-16	1024-1024-512-256-1	882.77 Million	16

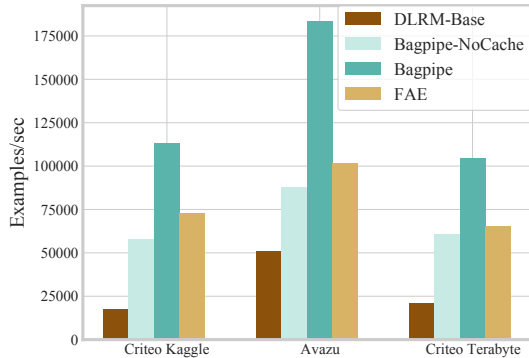


Figure 10: **Comparing BagPipe against existing systems:** We observe the BAGPIPE with caching provides upto $6.2\times$ speedup over DLRM and upto $1.75\times$ speedup over FAE. DLRM-Base here refers to publicly available implementation by Facebook.

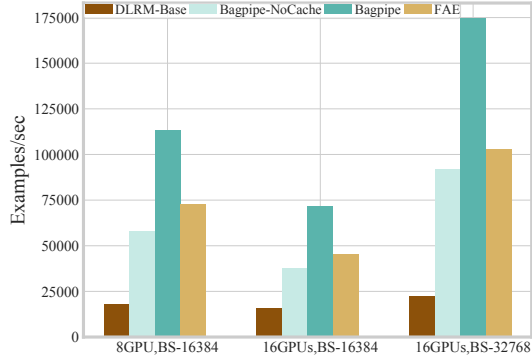


Figure 11: **Scalability of BagPipe:** We perform both weak and strong scaling on BAGPIPE. As we scale the benefits of BAGPIPE get higher. For 8GPUs, BAGPIPE provides a speedup of around $6\times$ over DLRM-Base while for 16 GPUs, it becomes around $7\times$. We use Criteo Kaggle dataset for these experiments.

with each datapoint. Table 2 also shows the total number of embeddings which will be required to represent the categorical features in the dataset. We also show the details of embedding dimensions and neural network dimension for DLRM in Table 2. These parameters are similar to the one used at Facebook [2].

Cluster Setup. We run all our experiments on Amazon Web Services. Our training machines are *p3.2xlarge* instances while our Embedding Server and Oracle Cacher are each hosted on a *c5.18xlarge* instance. Each *p3.2xlarge* instance contains NVidia V100 GPU and 8 CPU cores with 64 GB of memory. While each *C5.18xlarge* has 72 CPU cores and 144 GB of memory. For BAGPIPE we launched data loaders on the same *c5.18xlarge* as Oracle Cacher since the machine had ample compute.

BagPipe Configuration. Unless otherwise stated, for all our experiment we set the cache size such that we can perform a look-ahead of up to 200 batches. Further we also used a RPC batching parameter of 0.25 for eviction, which translates into cache evictions at the interval of every 50 iterations. We study the sensitivity of these parameters and effect on throughput and memory in Section 5.5. We run all our experiments for 2000 iterations, which roughly translates to 1 epoch on Criteo Kaggle Dataset with batch size of 16,384.

5.2 Comparison with existing systems

In Figure 10 we compare BAGPIPE against existing methods on three different datasets. For this experiment BAGPIPE used eight trainers each running on *p3.2xlarge* and one Oracle Cacher and Embedding Server which were launched on a single *c5.18xlarge*. We had data-processors running on the same machine as Oracle Cacher and we set the batch size for training as 16,384 which is similar to batch sizes used by MLPerf [33]. For DLRM [32] we used the existing open source implementation [35] provided by Facebook. Next we run BAGPIPE in three different modes, first we run BAGPIPE with no caching and prefetch, next we run BAGPIPE with both caching and pre-fetching enabled and lastly we run BAGPIPE with FAE [3] which uses static caching. We consistently observe BAGPIPE with caching is significantly faster than existing systems across all three datasets. Providing a speedup of upto $6.2\times$ over DLRM and upto $1.8\times$ over static caching approach proposed by FAE. We also observed that Facebook’s publicly available implementation

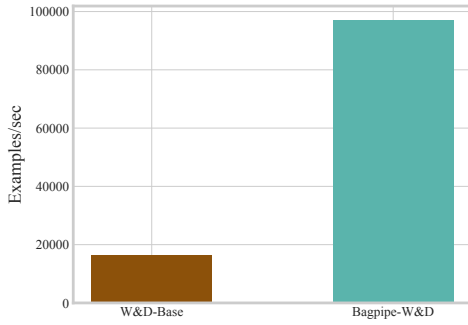


Figure 12: **Performance on Wide and Deep:** We compare BAGPIPE on W&D, using Criteo Kaggle dataset. For 8 trainer machines we found that BAGPIPE provides an overall speedup of $5.9\times$.

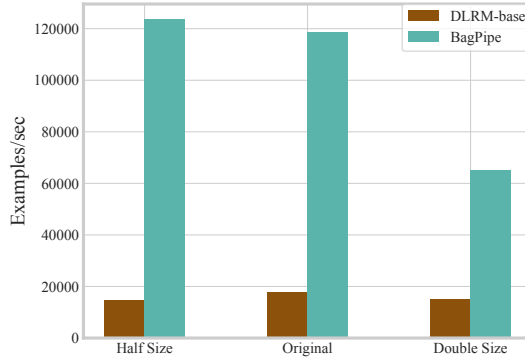


Figure 13: **Change in compute requirements of NN parameters** In this experiment we study how the scalability of BAGPIPE changes with increase in Dense Neural Network parameters. For this we changed the dense NN parameters given in Table 2, so *Half* refers to same number of layers just half the number of parameters. We see that as the compute requirements for the NN decrease, speedups provided by BAGPIPE increases.

spends almost 60% of time on data loading [47, 36]¹ and this leads to worse throughput compared to the BAGPIPE architecture. Finally, we observed that, FAE spent around 15% time on cache synchronization due to switching between hot and cold batches. For evaluation of FAE we did not include the pre-processing time needed by FAE for every new dataset.

We would like to point out that the majority of our time per iteration is spent on cache sync as shown in Figure 2. The primary reason for this is that *p3.2xlarge* machines only have a steady bandwidth of around 2.5Gbps and the total cache synchronization after every iteration is around 20MB. Out of this 4 Megabytes is synchronized on the critical path, rest we try to overlap with the forward pass. However due to limited bandwidth in our setup (2.5 Gbps) and very small forward time (10ms) we are not able to completely overlap our communication. We study this in more details in Section 5.5. With higher bandwidths or higher compute requirements (longer forward time) , our system will perform significantly better, as the cache sync time will reduce even further and a longer forward pass will provide an opportunity to overlap communication. From Figure 9 we also note that BAGPIPE embedding fetch/writeback is not on the critical path anymore.

5.3 Scalability of BagPipe

Next we perform both weak and strong scaling on BAGPIPE by increasing the number of GPUs to 16. For strong scaling we retain the batch size as 16,384 while for weak scaling we doubled the batch size to 32,768. Since training DLRMs is still network bound strong scaling reduces the compute per machine while increasing the amount of communication. In Figure 11 we observe a net overall slowdown across all three techniques when performing strong scaling. When going from 8 machines to 16 machines BAGPIPE’s throughput decreased by 36%. However BAGPIPE performs significantly better with weak scaling, when increasing batch size to 32,768 from 16,384 while increasing number of machines from 8 to 16 we observe that BAGPIPE’s throughput increases by 57%, however even in case of weak scaling the increase in throughput is sublinear due to communication overheads.

5.4 Comparing BagPipe on different models

We also compare BAGPIPE on other recommendation models. First we use Google’s Wide and Deep Network [6] architecture. Compared to DLRM, which has two MLPs, the Wide and Deep model only has one MLP layer and one linear layer. This translates into lower compute density then DLRMs. Figure 12 shows that BAGPIPE achieves around $5.9\times$ speedup compared to the Wide and Deep baseline.

¹this has been observed by prior work as well

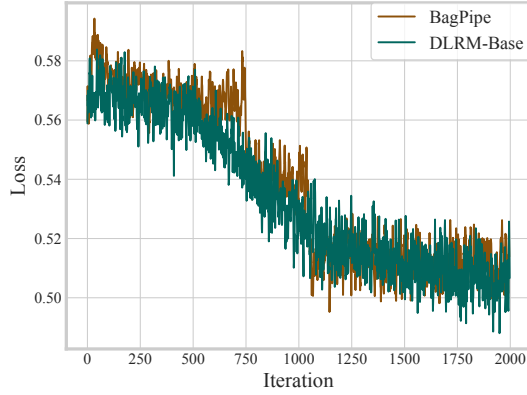


Figure 14: **Loss convergence for BagPipe and DLRM-Base:** We observed similar convergence of loss between BagPipe and DLRM-Base, with slight differences in value due to random initialization.

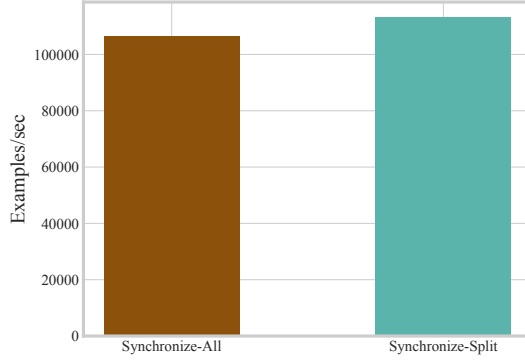


Figure 15: **Affect of splitting cache synchronization:** We compare the effect of splitting communication, using Kaggle Criteo dataset. We observed that splitting communication for the models we tried only provides around 6% speedup. This is primarily because the models we used did not perform enough compute to overlap.

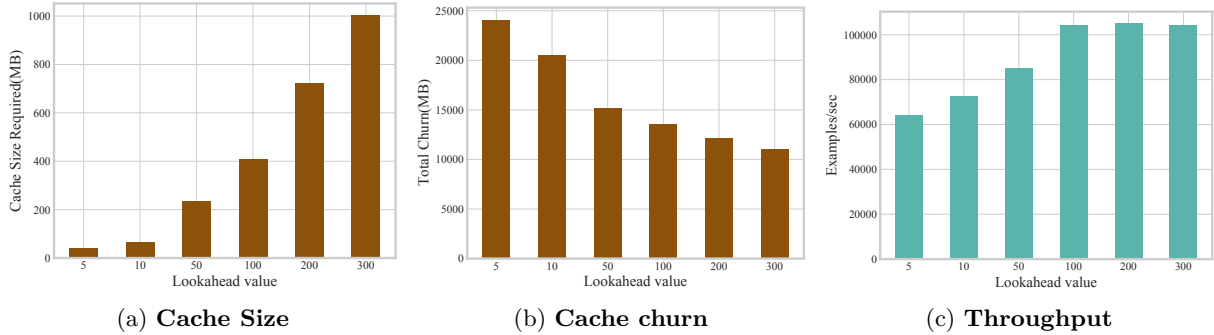


Figure 16: **Effect of increasing \mathcal{L} :** We study how changing \mathcal{L} effects Cache Size, Cache Churn and Throughput. We observe that with increase in \mathcal{L} the cache size required also increases, since we need the cache space to store the extra cold embeddings required by additional lookahead. Further with increase in \mathcal{L} the churn (sum of evictions and additions) also decreases. However, the gain in throughput plateaus after a \mathcal{L} of 100.

Next, we also study synthetic models by changing NN compute requirements and measure how this can effect the speedups provided by BAGPIPE. We study this with 8 *p3.2xlarge* GPUs on Criteo Kaggle dataset. We observe that as the compute requirements increase the comparative speedup provided by BAGPIPE decreases, *e.g.*, if we double the compute requirements of NN parameters from the one shown in Table 2, we see the speedup decreases from $6.2\times$ to $4.3\times$. If at the same time if we half the compute requirements, we observe that the speedup increases to $8\times$.

5.5 Sensitivity Analysis of BagPipe

In this section we study throughput of BAGPIPE with different look ahead value and configurations. We also micro-benchmark different components of BAGPIPE. Unless stated otherwise, for all these experiments we use 8 *p3.2xlarge* training machines and 2 *c5.8xlarge*, one as Oracle Cacher and one as Embedding Server, with data pre-processors operating on the same machine as Oracle Cacher.. Further, for all these experiments we used a global batch size of 16,384 and the Criteo Kaggle dataset.

Effect of \mathcal{L} . In Figure 16 we study how various system metrics are affected by \mathcal{L} . In Figure 16a we first examine how the amount of cache required changes for different look-ahead values, we observe that as the look-ahead value is increased, the cache size required keeps increasing sub-linearly. The sub-linearity comes from the fact that the extra batches looked ahead could reuse some of embeddings that were found in the previous batches.

Next we look at the churn from the cache for 1 epoch of training. We calculate the churn as the sum of

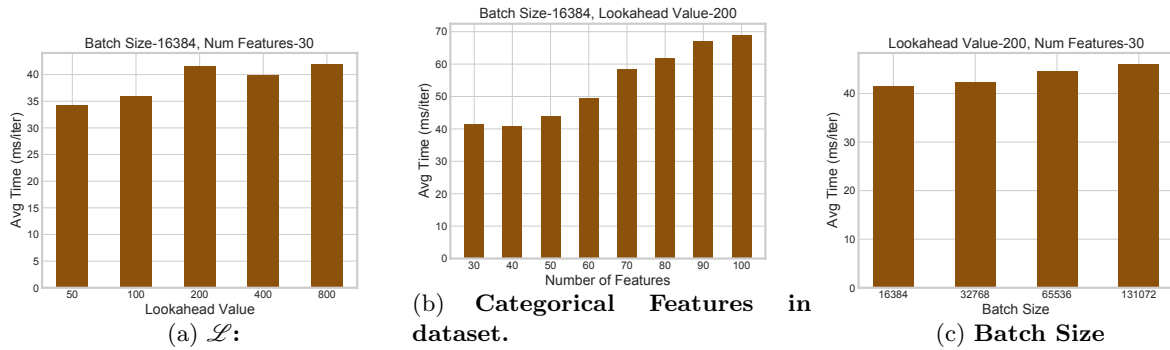


Figure 17: **Latency of Oracle Cacher**: We study how changes in \mathcal{L} , features in dataset and Batch Size effect latency of Oracle Cacher. Scalability of Oracle Cacher depends on these three parameters. We see that overall Oracle Cacher scales very well, for increasing \mathcal{L} and Batch Size it is close to constant, while increases sub linearly with number of features.

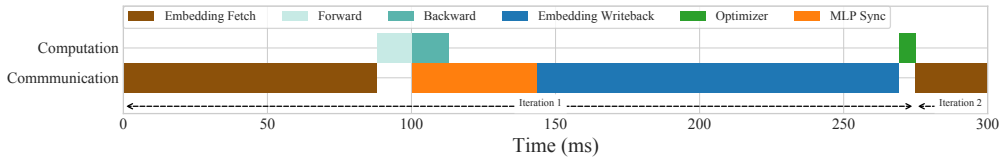


Figure 18: **Timeline of Operations performed by DLRM Baseline for first 300ms**: The above figure shows the various operations performed by DLRM baseline over the course of two iterations. We observe that DLRM baseline can only overlap the synchronization of MLP parameters with the backward pass. Rest of the operations are performed on the critical training path. Only around 8% of time per iteration is spent on compute.

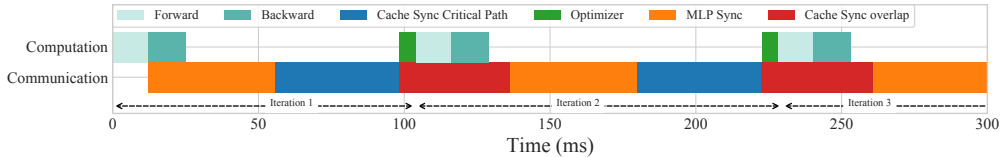


Figure 19: **Timeline of Operations performed by BagPipe for first 300ms**: The above figure shows the timeline of operations performed by BAGPIPE. We show that BAGPIPE has the potential to almost overlap large portions of communication with compute. However, since the compute performed by DLRM is only 30ms, we still see some portion of communication on the critical path. Further compared to DLRM baseline in Figure 18 we also don't have any embedding fetch operations in our critical path as they are handled by our dynamic cache and embedding prefetch.

evictions and additions to the cache during the whole training. In Figure 16b we observe that as look-ahead value is increased the churn decreases. This shows that when look-ahead value increases, the network traffic generated by cache evictions and additions will decrease.

Finally we look at how look-ahead value effects training throughput. In Figure 16c we observe that benefits from increasing look-ahead value start plateauing beyond look-ahead value of 100. This shows that increasing cache size/look-ahead value beyond a certain value leads to little or no speedups. This is because as the look-ahead value goes over 200, we are keeping all the elements which are popular in the cache and increasing \mathcal{L} at this point is not decreasing communication.

Overhead of Oracle Cacher. We benchmark the overhead of the operations of Oracle Cacher by changing different input features. Figure 17a, 17b, 17c shows the overhead of Oracle Cacher as we increase the \mathcal{L} , number of categorical features and batch size. We observe that for batch size and \mathcal{L} Oracle Cacher takes almost constant time to process, while increasing number of categorical features increases the overhead sub linearly. We will like to point out that as Oracle Cacher is overlapped with training, the latency requirement is that Oracle Cacher should take less time than the time taken for one training iteration. As long as this is the case, Oracle Cacher will not be the bottleneck.

Effect of splitting cache synchronization. As discussed in Section 3.2 for synchronizing caches we split the gradient update into two parts. First portion consists of gradient updates for the embeddings

which are needed for the next iteration, second portion consists of remaining gradients. The first portion is synchronized on the critical path and is a blocking operation. The second portion of the updates is performed asynchronously. This splitting of updates allows us to reduce the communication on the critical path and overlap large portion of synchronization with the forward pass. For Criteo kaggle dataset at batch size 16,384 we observed that only on avg 20 percent of updates have to be performed on critical path, *i.e.*, out of approximately 14,000 embedding updates only approximately 3,000 embeddings updates need to be synchronized before proceeding for the next iteration. In Figure 15 we observe that splitting only provides 6% speedup. The reason for this is that the models we have evaluated against have small computation footprint, while the instances we use (p3.2xlarge) have comparatively low bandwidth (2.5 Gbps) thus limiting the opportunity to overlap. We show a timeline of operations performed by BAGPIPE in Figure 19 and by the DLRM baseline in Figure 18. We observe that BAGPIPE is network-bound and even though there are operations that can be potentially overlapped, BAGPIPE is currently not able to hide all the communication costs. As more computationally expensive recommendation models [17, 6] are used, or higher bandwidth becomes available our optimizations will provide better gains.

Convergence Comparison. Since, we have made no changes to the training process itself, we should observe the same convergence properties. In Figure 14 we verify that BAGPIPE’s convergence curve is almost the same as DLRM-Base curve, the minor differences arise from randomization.

6 Related Work

Speeding up training for recommendation engines recommendation has seen interest from both machine learning and systems community. As discussed in Section 2.2 the closest work to ours is the Frequent Access Embedding (FAE) framework [3]. We have provided several qualitative reasons as well have extensively compared quantitatively against this work 5.2. Prior work [45, 19] uses Near Data Processing to try to reduce the overhead of embedding fetch by offloading some portion of the compute to the storage hardware DRAM and SSD. These optimizations are orthogonal to optimizations introduced by BAGPIPE and can be used to further improve scalability of BAGPIPE. Recent [46] work aims to reduce the size of embedding tables by using Tensor compression. They show that by increasing some compute they can reduce the size of embedding tables by almost 200x. Similar work by [12] performs gradient compression on the updates to embedding table to reduce the time spent in gradient synchronization. These approaches change the training algorithm to achieve the said gains which can lead to accuracy loss. These algorithms can be implemented in BAGPIPE and used to speed up training. In [14] the authors propose a method to reduce the accuracy loss because of asynchronous training, by creating partitioning workers and keeping the workers in a partition synchronised. We on the other hand implement only synchronous training. A very recent work by [27] introduces a new hybrid sync-async algorithm to train recommender models, unlike this work we only focus on synchronous training. [47] proposes methods for improving data processing while training recommender systems. We use their insight in designing the data pre-processing module of BAGPIPE.

Several other works have looked at speeding up distributed large parameter DNN training, [31] introduce pipeline parallelism. While, Gshard [23] shards massive language models across several different workers. Flexflow [18] tries to find the best parallelization strategy across training workers to provide best throughput. Work by [25] improves scalability of data parallel training by overlapping computation with communication. All these approaches have been designed specifically for dense language and vision models. None of these approaches are directly applicable to recommender system training.

7 Conclusion

BAGPIPE is a new dis-aggregated architecture for training deep learning based recommendation models. The optimizations used by BAGPIPE are completely transparent to the user and the gains achieved by BAGPIPE are through better resource utilization and overlapping of computation with data movement. BAGPIPE by allowing independent scaling of resources for different portions of recommendation model for better resource utilization. And by using the idea of caching and prefetching to remove the embedding access from the critical path, BAGPIPE provides an end to end speedup of upto $6\times$ when compared against state of the art baselines.

References

- [1] Mpi all to all. https://www.rookiehpc.com/mpi/docs/mpi_alltoall.php, 2019. Accessed: December 12, 2022.
- [2] Bilge Acun, Matthew Murphy, Xiaodong Wang, Jade Nie, Carole-Jean Wu, and Kim Hazelwood. Understanding training efficiency of deep learning recommendation models at scale. In *2021 IEEE International Symposium on High-Performance Computer Architecture (HPCA)*, pages 802–814. IEEE.
- [3] Muhammad Adnan, Yassaman Ebrahimzadeh Maboud, Divya Mahajan, and Prashant J Nair. High-performance training by exploiting hot-embeddings in recommendation systems. *arXiv preprint arXiv:2103.00686*, 2021.
- [4] Michael Armbrust, Ali Ghodsi, Reynold Xin, and Matei Zaharia. Lakehouse: a new generation of open platforms that unify data warehousing and advanced analytics. In *Proceedings of CIDR*, 2021.
- [5] Laszlo A. Belady. A study of replacement algorithms for a virtual-storage computer. *IBM Systems journal*, 5(2):78–101, 1966.
- [6] Heng-Tze Cheng, Levent Koc, Jeremiah Harmsen, Tal Shaked, Tushar Chandra, Hrishi Aradhye, Glen Anderson, Greg Corrado, Wei Chai, Mustafa Ispir, et al. Wide & deep learning for recommender systems. In *Proceedings of the 1st workshop on deep learning for recommender systems*, pages 7–10, 2016.
- [7] Paul Covington, Jay Adams, and Emre Sargin. Deep neural networks for youtube recommendations. In *Proceedings of the 10th ACM conference on recommender systems*, pages 191–198, 2016.
- [8] Benoit Dageville, Thierry Cruanes, Marcin Zukowski, Vadim Antonov, Artin Avanes, Jon Bock, Jonathan Claybaugh, Daniel Engovatov, Martin Hentschel, Jiansheng Huang, et al. The snowflake elastic data warehouse. In *Proceedings of the 2016 International Conference on Management of Data*, pages 215–226, 2016.
- [9] Shuiguang Deng, Longtao Huang, Guandong Xu, Xindong Wu, and Zhaozhui Wu. On deep learning for trust-aware recommendations in social networks. *IEEE transactions on neural networks and learning systems*, 28(5):1164–1177, 2016.
- [10] Udit Gupta, Samuel Hsia, Vikram Saraph, Xiaodong Wang, Brandon Reagen, Gu-Yeon Wei, Hsien-Hsin S Lee, David Brooks, and Carole-Jean Wu. Deeprecsys: A system for optimizing end-to-end at-scale neural recommendation inference. In *2020 ACM/IEEE 47th Annual International Symposium on Computer Architecture (ISCA)*, pages 982–995. IEEE, 2020.
- [11] Udit Gupta, Carole-Jean Wu, Xiaodong Wang, Maxim Naumov, Brandon Reagen, David Brooks, Bradford Cottel, Kim Hazelwood, Mark Hempstead, Bill Jia, et al. The architectural implications of facebook’s dnn-based personalized recommendation. In *2020 IEEE International Symposium on High Performance Computer Architecture (HPCA)*, pages 488–501. IEEE, 2020.
- [12] Vipul Gupta, Dhruv Choudhary, Peter Tang, Xiaohan Wei, Xing Wang, Yuzhen Huang, Arun Kejariwal, Kannan Ramchandran, and Michael W Mahoney. Training recommender systems at scale: Communication-efficient model and data parallelism. In *Proceedings of the 27th ACM SIGKDD Conference on Knowledge Discovery & Data Mining*, pages 2928–2936, 2021.
- [13] Xiangnan He, Lizi Liao, Hanwang Zhang, Liqiang Nie, Xia Hu, and Tat-Seng Chua. Neural collaborative filtering. In *Proceedings of the 26th international conference on world wide web*, pages 173–182, 2017.
- [14] Yuzhen Huang, Xiaohan Wei, Xing Wang, Jiyan Yang, Bor-Yiing Su, Shivam Bharuka, Dhruv Choudhary, Zewei Jiang, Hai Zheng, and Jack Langman. Hierarchical training: Scaling deep recommendation models on large cpu clusters. In *Proceedings of the 27th ACM SIGKDD Conference on Knowledge Discovery & Data Mining*, KDD ’21, page 3050–3058, New York, NY, USA, 2021. Association for Computing Machinery.

- [15] Wen-mei Hwu and Yale N Patt. Hpsm, a high performance restricted data flow architecture having minimal functionality. *ACM SIGARCH Computer Architecture News*, 14(2):297–306, 1986.
- [16] Avazu Inc. Avazu click logs. <https://www.kaggle.com/c/avazu-ctr-prediction/data>, 2013. Accessed: December 10, 2020.
- [17] Tigran Ishkhanov, Maxim Naumov, Xianjie Chen, Yan Zhu, Yuan Zhong, Alisson Gusatti Azzolini, Chonglin Sun, Frank Jiang, Andrey Malevich, and Liang Xiong. Time-based sequence model for personalization and recommendation systems. *arXiv preprint arXiv:2008.11922*, 2020.
- [18] Zhihao Jia, Sina Lin, Charles R Qi, and Alex Aiken. Exploring hidden dimensions in parallelizing convolutional neural networks. *arXiv preprint arXiv:1802.04924*, 2018.
- [19] Liu Ke, Udit Gupta, Benjamin Youngjae Cho, David Brooks, Vikas Chandra, Utku Diril, Amin Firoozshahian, Kim Hazelwood, Bill Jia, Hsien-Hsin S Lee, et al. Recnmp: Accelerating personalized recommendation with near-memory processing. In *2020 ACM/IEEE 47th Annual International Symposium on Computer Architecture (ISCA)*, pages 790–803. IEEE, 2020.
- [20] Criteo Labs. Criteo kaggle logs. <https://labs.criteo.com/2014/02/kaggle-display-advertising-challenge-dataset/>, 2013. Accessed: December 10, 2020.
- [21] Criteo Labs. Terabyte click logs. <https://labs.criteo.com/2014/02/kaggle-display-advertising-challenge-dataset/>, 2013. Accessed: December 10, 2020.
- [22] Joonseok Lee, Sami Abu-El-Haija, Balakrishnan Varadarajan, and Apostol Natsev. Collaborative deep metric learning for video understanding. In *Proceedings of the 24th ACM SIGKDD International Conference on Knowledge Discovery & Data Mining*, pages 481–490, 2018.
- [23] Dmitry Lepikhin, HyoukJoong Lee, Yuanzhong Xu, Dehao Chen, Orhan Firat, Yanping Huang, Maxim Krikun, Noam Shazeer, and Zhifeng Chen. Gshard: Scaling giant models with conditional computation and automatic sharding. *arXiv preprint arXiv:2006.16668*, 2020.
- [24] Pengcheng Li, Runze Li, Qing Da, An-Xiang Zeng, and Lijun Zhang. Improving multi-scenario learning to rank in e-commerce by exploiting task relationships in the label space. In *Proceedings of the 29th ACM International Conference on Information & Knowledge Management*, pages 2605–2612, 2020.
- [25] Shen Li, Yanli Zhao, Rohan Varma, Omkar Salpekar, Pieter Noordhuis, Teng Li, Adam Paszke, Jeff Smith, Brian Vaughan, Pritam Damania, et al. Pytorch distributed: Experiences on accelerating data parallel training. *arXiv preprint arXiv:2006.15704*, 2020.
- [26] Zhi Li, Hongke Zhao, Qi Liu, Zhenya Huang, Tao Mei, and Enhong Chen. Learning from history and present: Next-item recommendation via discriminatively exploiting user behaviors. In *Proceedings of the 24th ACM SIGKDD International Conference on Knowledge Discovery & Data Mining*, pages 1734–1743, 2018.
- [27] Xiangru Lian, Binhang Yuan, Xuefeng Zhu, Yulong Wang, Yongjun He, Honghuan Wu, Lei Sun, Haodong Lyu, Chengjun Liu, Xing Dong, et al. Persia: A hybrid system scaling deep learning based recommenders up to 100 trillion parameters. *arXiv preprint arXiv:2111.05897*, 2021.
- [28] David C Liu, Stephanie Rogers, Raymond Shiau, Dmitry Kislyuk, Kevin C Ma, Zhigang Zhong, Jenny Liu, and Yushi Jing. Related pins at pinterest: The evolution of a real-world recommender system. In *Proceedings of the 26th international conference on world wide web companion*, pages 583–592, 2017.
- [29] McKinsey and Company. How retailers can keep up with consumers. <https://www.mckinsey.com/industries/retail/our-insights/how-retailers-can-keep-up-with-consumers>, 2013. Accessed: December 11, 2021.
- [30] Dheevatsa Mudigere, Yuchen Hao, Jianyu Huang, Zhihao Jia, Andrew Tulloch, Srinivas Sridharan, Xing Liu, Mustafa Ozdal, Jade Nie, Jongsoo Park, Liang Luo, Jie Amy Yang, Leon Gao, Dmytro Ivchenko, Aarti Basant, Yuxi Hu, Jiyan Yang, Ehsan K. Ardestani, Xiaodong Wang, Rakesh Komuravelli, Ching-Hsiang Chu, Serhat Yilmaz, Huayu Li, Jiyuan Qian, Zhuobo Feng, Yinbin Ma, Junjie Yang, Ellie Wen,

- Hong Li, Lin Yang, Chonglin Sun, Whitney Zhao, Dmitry Melts, Krishnaveni Dhulipala, Kranthi G. Kishore, Tyler Graf, Assaf Eisenman, Kiran Kumar Matam, Adi Gangidi, Guoqiang Jerry Chen, Manoj Krishnan, Avinash Nayak, Krishnakumar Nair, Bharath Muthiah, Mahmoud khorashadi, Pallab Bhat-tacharya, Petr Lapukhov, Maxim Naumov, Ajit Mathews, Lin Qiao, Mikhail Smelyanskiy, Bill Jia, and Vijay Rao. Software-hardware co-design for fast and scalable training of deep learning recommendation models. 2021.
- [31] Deepak Narayanan, Aaron Harlap, Amar Phanishayee, Vivek Seshadri, Nikhil R Devanur, Gregory R Ganger, Phillip B Gibbons, and Matei Zaharia. Pipedream: generalized pipeline parallelism for dnn training. In *Proceedings of the 27th ACM Symposium on Operating Systems Principles*, pages 1–15, 2019.
 - [32] Maxim Naumov, Dheevatsa Mudigere, Hao-Jun Michael Shi, Jianyu Huang, Narayanan Sundaraman, Jongsoo Park, Xiaodong Wang, Udit Gupta, Carole-Jean Wu, Alisson G Azzolini, et al. Deep learning recommendation model for personalization and recommendation systems. *arXiv preprint arXiv:1906.00091*, 2019.
 - [33] Nvidia. Nvidia mlperf. <https://developer.nvidia.com/blog/introducing-merlin-hugectr-training-framework-dedicated-to-recommender-systems/>, 2019. Accessed: December 10, 2021.
 - [34] PyTorch. Embedding bag. <https://pytorch.org/docs/stable/generated/torch.nn.EmbeddingBag.html>, 2019. Accessed: December 12, 2021.
 - [35] Facebook Research. Facebook research dlrm. <https://github.com/facebookresearch/dlrm>, 2019. Accessed: December 10, 2021.
 - [36] Facebook Research. Facebook research dlrm. <https://github.com/facebookresearch/dlrm/issues/206>, 2019. Accessed: December 10, 2021.
 - [37] Yuhan Su, Zhongming Jin, Ying Chen, Xinghai Sun, Yaming Yang, Fangzheng Qiao, Fen Xia, and Wei Xu. Improving click-through rate prediction accuracy in online advertising by transfer learning. In *Proceedings of the International Conference on Web Intelligence*, pages 1018–1025, 2017.
 - [38] Yong Kiam Tan, Xinxing Xu, and Yong Liu. Improved recurrent neural networks for session-based recommendations. In *Proceedings of the 1st workshop on deep learning for recommender systems*, pages 17–22, 2016.
 - [39] Trinh Xuan Tuan and Tu Minh Phuong. 3d convolutional networks for session-based recommendation with content features. In *Proceedings of the eleventh ACM conference on recommender systems*, pages 138–146, 2017.
 - [40] Bartłomiej Twardowski. Modelling contextual information in session-aware recommender systems with neural networks. In *Proceedings of the 10th ACM Conference on Recommender Systems*, pages 273–276, 2016.
 - [41] Aäron Van Den Oord, Sander Dieleman, and Benjamin Schrauwen. Deep content-based music recommendation. In *Neural Information Processing Systems Conference (NIPS 2013)*, volume 26. Neural Information Processing Systems Foundation (NIPS), 2013.
 - [42] Suhang Wang, Yilin Wang, Jiliang Tang, Kai Shu, Suhas Ranganath, and Huan Liu. What your images reveal: Exploiting visual contents for point-of-interest recommendation. In *Proceedings of the 26th international conference on world wide web*, pages 391–400, 2017.
 - [43] Xinxi Wang and Ye Wang. Improving content-based and hybrid music recommendation using deep learning. In *Proceedings of the 22nd ACM international conference on Multimedia*, pages 627–636, 2014.
 - [44] Jiqing Wen, James She, Xiaopeng Li, and Hui Mao. Visual background recommendation for dance performances using deep matrix factorization. *ACM Transactions on Multimedia Computing, Communications, and Applications (TOMM)*, 14(1):1–19, 2018.

- [45] Mark Wilkening, Udit Gupta, Samuel Hsia, Caroline Trippel, Carole-Jean Wu, David Brooks, and Gu-Yeon Wei. Recssd: near data processing for solid state drive based recommendation inference. In *Proceedings of the 26th ACM International Conference on Architectural Support for Programming Languages and Operating Systems*, pages 717–729, 2021.
- [46] Chunxing Yin, Bilge Acun, Carole-Jean Wu, and Xing Liu. Tt-rec: Tensor train compression for deep learning recommendation models. In A. Smola, A. Dimakis, and I. Stoica, editors, *Proceedings of Machine Learning and Systems*, volume 3, pages 448–462, 2021.
- [47] Mark Zhao, Niket Agarwal, Aarti Basant, Bugra Gedik, Satadru Pan, Mustafa Ozdal, Rakesh Komuravelli, Jerry Pan, Tianshu Bao, Haowei Lu, et al. Understanding and co-designing the data ingestion pipeline for industry-scale recsys training. *arXiv preprint arXiv:2108.09373*, 2021.